Nanoscale

Cite this: *Nanoscale*, 2012, **4**, 6637

www.rsc.org/nanoscale

PAPER

Wafer-scale MoS_2 thin layers prepared by MoO_3 sulfurization†

Yu-Chuan Lin,‡[a] Wenjing Zhang,‡[a] Jing-Kai Huang,[ab] Keng-Ku Liu,[a] Yi-Hsien Lee,[a] Chi-Te Liang,[c] Chih-Wei Chu[d] and Lain-Jong Li*[ae]

Received 12th July 2012, Accepted 26th August 2012
DOI: 10.1039/c2nr31833d

Atomically thin molybdenum disulfide (MoS_2) layers have attracted great interest due to their direct-gap property and potential applications in optoelectronics and energy harvesting. Meanwhile, they are extremely bendable, promising for applications in flexible electronics. However, the synthetic approach to obtain large-area MoS_2 atomic thin layers is still lacking. Here we report that wafer-scale MoS_2 thin layers can be obtained using MoO_3 thin films as a starting material followed by a two-step thermal process, reduction of MoO_3 at 500 °C in hydrogen and sulfurization at 1000 °C in the presence of sulfur. Spectroscopic, optical and electrical characterizations reveal that these films are polycrystalline and with semiconductor properties. The obtained MoS_2 films are uniform in thickness and easily transferable to arbitrary substrates, which make such films suitable for flexible electronics or optoelectronics.

1. Introduction

Graphene has attracted much attention due to its unique chemical structure, two-dimensionality and physical properties such as high carrier mobility and excellent sensitivity.[1] These properties make it a good candidate for high-frequency devices[2] and biosensor applications.[3,4] However, the gapless nature of graphene[5] slows its development in logic circuit applications. Other types of two-dimensional layered nanomaterials, transition-metal dichalcogenides, also show great potential in nanoelectronics and optical application.[6–9] In particular, atomically thin molybdenum disulfide (MoS_2) layers have drawn great interest because they exhibit many desirable physical properties. When the dimension of MoS_2 is reduced from a three-dimensional bulk form into a two-dimensional sheet, the band gap transforms from an indirect to a direct one.[10,11] Recently, exfoliated MoS_2 atomic thin layers have been fabricated into transistors which demonstrate excellent on/off current ratios and high carrier mobility, promising for low power electronics.[12] Several methods have been proposed to prepare MoS_2 atomic thin layers, including scotch tape assisted micromechanical exfoliation,[8–11,13] intercalation assisted exfoliation,[14–21] solution exfoliation,[6,16,17,22,23] physical vapor deposition,[24,25] hydrothermal synthesis,[26] electrochemical synthesis,[27,28] sulfurization of molybdenum oxides[29,30] and thermolysis of a precursor containing Mo and S atoms.[23] Most of these methods may produce good quality of MoS_2 layers but the lateral dimensions are in the range of several to several tens of micrometers, which are not suitable for use in large area electronics. Methods to synthesize highly uniform and large area MoS_2 thin films with ideal electrical performance is still limited since MoS_2 tends to form nanoparticles or nanotube structures during the synthesis.[31] Thus, wafer-scale synthesis of highly uniform thin MoS_2 films on insulating substrates is desirable. Zhan *et al.* have reported a method to obtain MoS_2 layers by direct sulfurization of Mo metal thin films,[32] where the obtained MoS_2 shows resistor-like behavior. In this contribution, we report that wafer-scale MoS_2 thin layers can be obtained by a two-step thermal process[33] to convert a MoO_3 thin layer to a MoS_2 thin layer. Spectroscopic, optical and electrical characterizations reveal that these films are polycrystalline and with semiconductor behaviors. The MoS_2 films obtained are uniform in thickness and are easily transferable to arbitrary substrates, which make such films favorable for flexible electronics or optoelectronics.

2. Experimental section

2.1 Synthesis of thin-layer MoS_2

MoO_3 (molybdenum(VI) oxide) powder was purchased from Alfa Aesar (99.998%). MoO_3 thin films with desired thickness were thermally deposited on a *c*-face sapphire substrate at a rate of 0.5 A s^{-1} by a thermal evaporator, where the sapphire substrate was cleaned with a standard piranha solution prior to the

[a]*Institute of Atomic and Molecular Sciences, Academia Sinica, Taipei, 10617, Taiwan. E-mail: lanceli@gate.sinica.edu.tw*
[b]*Department of Photonics, National Chiao Tung University, HsinChu 300, Taiwan*
[c]*Department of Physics, National Taiwan University, Taipei 106, Taiwan*
[d]*Research Center for Applied Sciences, Academia Sinica, Taipei, 11529, Taiwan*
[e]*Department of Physics, National Tsing Hua University, HsinChu 300, Taiwan*

† Electronic supplementary information (ESI) available. See DOI: 10.1039/c2nr31833d

‡ These authors contributed equally.

deposition of MoO_3. The MoO_3 film coated on a *c*-face sapphire substrate was placed in the cold zone of the quartz tube flowing with an Ar–H_2 mixture (flow rate = 4 : 1; 1 Torr). When the centre of the furnace reached 500 °C, the substrate was moved to the hot zone of the furnace for the first annealing. The chamber was kept at a low pressure (1 Torr) in an Ar–H_2 atmosphere (flow rate 4 : 1). After 1 h, the sample was moved to the cold zone and sulfur powder loaded in a ceramic boat was placed in the cold zone in the furnace. Then the samples together with the sulfur boat were moved to the centre of the furnace again for the second annealing after the hot zone reached 1000 °C. The substrate was heated to 1000 °C at a rate of 15 °C min^{-1}. The sample was kept at 1000 °C for 30 min using 70 sccm Ar as carrier and protection gas (pressure: 600 Torr). After this, the heater of the furnace was turned off, and the sample was left in the chamber to cool down to room temperature.

2.2 Transfer of MoS_2 onto fresh SiO_2/Si or other substrates

To transfer as-grown MoS_2 onto fresh SiO_2 (300 nm)/Si substrates, the MoS_2 film was coated with a layer of poly(methyl methacrylate) (PMMA) (Micro Chem. 950K A4) by spin-coating (step 1: 500 rpm for 10 s; step 2: 3000 rpm for 60 s), followed by baking at 100 °C for 10 min. After that, the PMMA-capped MoS_2 was then put into a NaOH (2 M) solution at 100 °C for 30 min. The PMMA-supported MoS_2 film was then transferred to deionized (DI) water to remove the etchant and residues. A fresh SiO_2/Si substrate was then used to "fish out" the PMMA-capped MoS_2 film, followed by drying on a hot-plate (100 °C for 10 min). The PMMA was removed by acetone, isopropyl alcohol (IPA), followed by DI water and chloroform rinsing.

2.3 Characterization

The AFM images were taken in a Veeco Dimension-Icon system. The scanning rate was 0.976 Hz with 512 scanning lines. Raman spectra were collected in a NT-MDT confocal Raman microscopic system (exciting laser wavelength 473 nm and laser spot-size of ~0.5 μm). The Si peak at 520 cm^{-1} was used as reference for wavenumber calibration in Raman characterization. Photoluminescence (PL) measurements were performed with excitation from a solid-state 473 nm laser with a power of 500 μW. The laser radiation was focused onto the MoS_2 sheets with a spot-size around 0.5 μm. The nanostructure of MoS_2 sheets was investigated in a JEOL-2010F TEM with accelerating voltage of 200 keV. Chemical configurations were determined by X-ray photoelectron spectroscopy (XPS, Phi V6000). XPS measurements were performed with an Mg-Kα X-ray source on the samples. The energy calibrations were made against the C 1s peak to eliminate the charging of the sample during analysis. The field-effect transistor device was fabricated by evaporating Au electrodes (80 nm thick) directly on top of the selected, regularly shaped graphene sheets using a copper grid (200 mesh, 20 μm spacing) as a hardmask. The typically obtained channel length between source and drain electrodes was around 20 μm. The electrical measurements were performed in ambient conditions using a Keithley semiconductor parameter analyzer, model 4200.

3. Results and discussion

A schematic illustration for the synthesis of thin MoS_2 layers is shown in Fig. 1a. A layer of MoO_3 (3.6 nm thick) was deposited on a clean *c*-phase sapphire substrate by thermal evaporation with a deposition rate of 0.05 nm s^{-1}. The MoO_3-coated sapphire substrate was first reduced to MoO_2 or other reduced forms in a hydrogen/Ar environment at 500 °C for 1 h.[34] The sample was then annealed in a sulfur-rich environment at 1000 °C for 30 min, where the chamber pressure was kept at 600 Torr and Ar was used as a dilute gas during the reaction. The approach is simple and scalable to wafer-size fabrication. It is noteworthy to point out that we have attempted the one-step direct sulfurization of MoO_3 with sulfur at 1000 °C, where the obtained MoS_2 films exhibited semiconductor properties, but the electrical carrier mobility was at least one order of magnitude lower than that from the two-step thermal process. The chemical equations for the two-step reaction are proposed in eqn (1) and (2).

$$MoO_{3(s)} + H_{2(g)} \rightarrow MoO_{2(s)} + H_2O_{(g)} \quad (1)$$

$$MoO_{2(s)} + 2S_{(g)} \rightarrow MoS_{2(s)} + O_{2(g)} \quad (2)$$

Fig. 1b shows a photograph for the MoS_2 thin layer grown on a 2 inch sapphire wafer, where the MoS_2 layer is continuous and uniformly flat across the wafer. The root-mean-square surface roughness measured by atomic force microscopy (AFM) is around 0.2 nm as shown in Fig. 1c. To estimate the thickness of the synthesized MoS_2 film, AFM was used to analyze the topography of an area with an occasionally found void as shown in Fig. 1d, where the cross-sectional height profiles for several randomly selected traces (indicated as white lines) show that the thickness of the MoS_2 layer ranges from 1.8 to 2.0 nm. The cross-sectional profile for one of the traces is shown in Fig. 1e. Additional AFM images are provided in Fig. S1 (ESI†).

Tunnelling electron microscopy (TEM) was used to further examine the layer number of the obtained wafer-scale MoS_2 thin films discussed in Fig. 1. The low-magnification TEM image in Fig. 2a shows the MoS_2 film on TEM grids and some wrinkles are evident on the edge of the film. These wrinkles were caused by the unavoidable film folding after the mechanical scratching during the TEM sample preparation. Three MoS_2 layers, where each layer is ~0.65 nm thick are identified at the wrinkled area in Fig. 2b, providing direct evidence that the synthesized films are trilayer MoS_2. The TEM images in Fig. 2c and d show the large-scale view for the MoS_2 film. The typical high-resolution TEM image for the MoS_2 layer is shown in Fig. 2e, where the periodic atom arrangements suggest that the MoS_2 layer is polycrystalline. The inset of Fig. 2e displays the selected area electron diffraction (SAED) pattern for the sample taken with an aperture size (~160 nm), and the points arranged in multiple hexagons also suggests that the MoS_2 layer stacking is polycrystalline. The TEM sample was transferred onto the TEM grid from a sapphire substrate by mechanical scratching and thus we can occasionally find monolayer MoS_2 on TEM grids. Fig. 2f shows the TEM and SAED pattern for the monolayer MoS_2 area, where the diffraction points (110) and (100) are indicated. Meanwhile, the lattice spacing of 0.27 and 0.16 nm corresponding to the (100) and (110) planes are indicated. These results

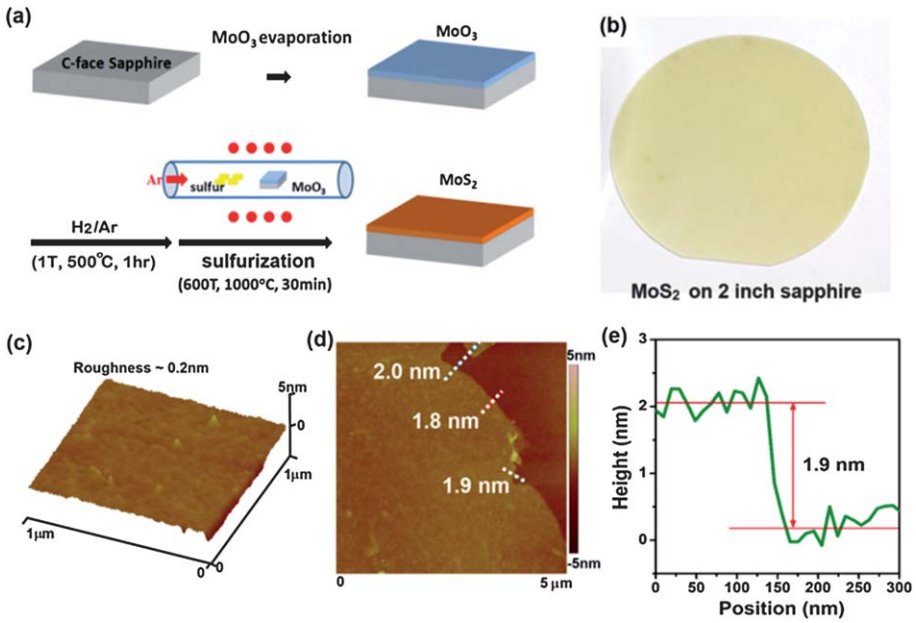

Fig. 1 (a) Schematic illustration for the synthesis of MoS_2 layers by MoO_3 sulfurization. A layer of MoO_3 (~3.6 nm) was thermally evaporated on the sapphire substrate. The MoO_3 was then converted to a MoS_2 by a two-step thermal process. (b) MoS_2 layer grown on a sapphire wafer. (c and d) Surface topographic images obtained by AFM. (e) A selected cross-sectional height profile showing the thickness of the MoS_2 layer.

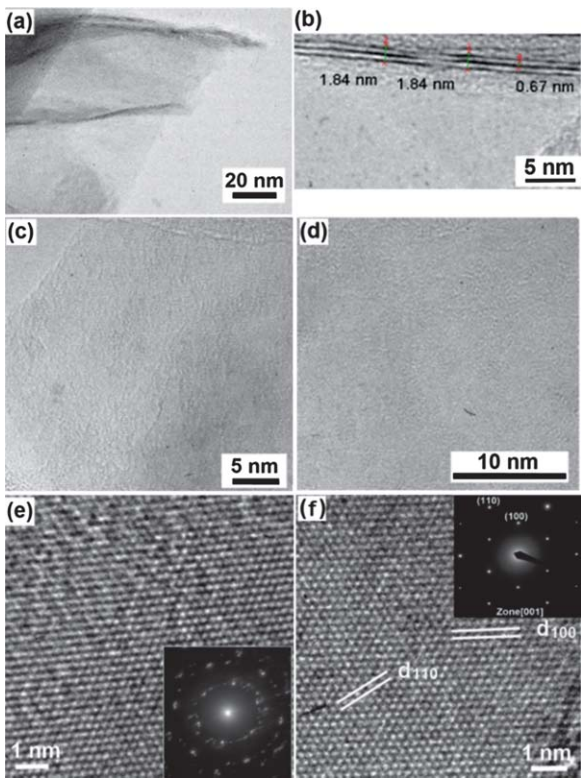

Fig. 2 (a and b) Low-magnification TEM images of the MoS_2 layers. The folded area at the edge clearly shows that the film is a MoS_2 trilayer and the distance between each layer is 0.65 nm. (c and d) TEM images show the large-area view of the film, where polycrystalline structures can be identified. (e) Typical high-resolution TEM image and SAED pattern for the trilayer MoS_2 film. (f) Selected high-resolution image and SAED pattern for the single-layer MoS_2.

further corroborate that the MoS_2 grown by the method is crystalline.

Fig. 3a and b display detailed X-ray photoemission spectroscopy (XPS) scans for the Mo and S binding energies of the MoO_3 layer before and after sulfurization. The survey scans are provided in Fig. S2 (ESI†). The MoO_3 layer exhibits two characteristic peaks at 235.5 and 232.2 eV, attributed to the $3d_{3/2}$ and $3d_{5/2}$ binding energies for Mo^{6+}. After sulfurization, the Mo 3d peaks are observed at 232.5 and 229.3 eV, assigned to the doublet

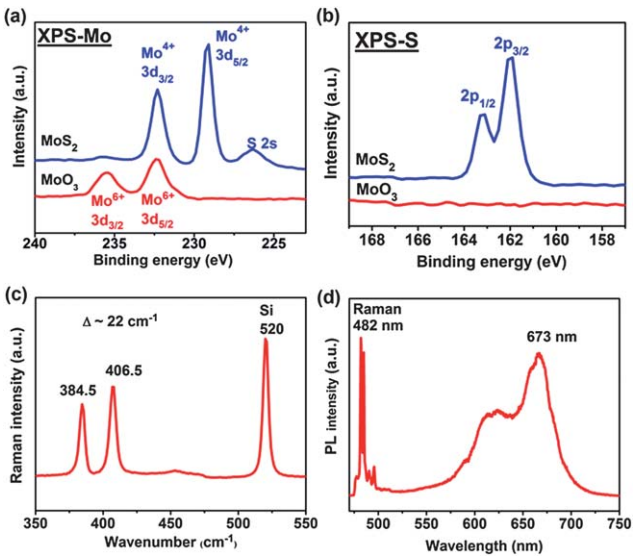

Fig. 3 X-Ray photoemission spectroscopy scans for (a) Mo and (b) S binding energies of the MoO_3 layer before and after sulfurization. (c) Raman and (d) photoluminescence spectra for the obtained MoS_2 trilayer after MoO_3 sulfurization.

Mo $d_{3/2}$ and Mo $d_{5/2}$ for Mo^{4+}. The stoichiometric ratio (S : Mo) estimated from the respective integrated peak area of XPS spectra is close to ~2. The result further confirms the formation of MoS_2. Fig. 3c and d show the Raman spectra and photoluminescence (PL) spectra for a MoS_2 trilayer, respectively. The excitation source is a laser with a wavelength of 473 nm. The Raman characteristic peaks at 403.8 and 358.8 cm^{-1} correspond to the A_{1g} and E_{2g} modes, respectively. The PL spectrum in Fig. 3d shows two main emission peaks at 627 and 673 nm, in good agreement with other reports for MoS_2 thin sheets obtained from exfoliation methods. These emissions are the A1 and B1 direct excitonic transitions as reported elsewhere.[10] Fig. S3 (ESI†) shows the absorption spectrum for the MoS_2 film where we also observe the A1 and B1 absorption peaks.

To access the homogeneity of the MoS_2 thin layers across the wafer, the MoS_2 film on a 2 inch sapphire wafer was divided into several areas, and numbers are labelled at the sites as in Fig. 4a. Raman spectra were taken at each numbered site. The energy difference between A_{1g} and E_{2g} Raman peaks (Δ) has been found to relate to the number of MoS_2 layers.[35] In Fig. 4b, we plot the statistical values as a function of numbered site (as indicated in Fig. 4a), where the variation of Δ is reasonably small (within 0.5 cm^{-1}) across the whole wafer. It is known that the peak width of the Raman peak is also sensitive to the crystalline quality of the MoS_2 layers.[33] The full width at half maximum (FWHM) of the E_{2g} peak as a function of numbered site is shown in Fig. 4b, where the variation also consistently suggests that the as-grown MoS_2 wafer layers exhibit good uniformity. In addition to the statistical measurements, we have also performed PL and Raman mappings for a 50 μm × 50 μm square area and the results shown in Fig. S4 and S5 (ESI†) demonstrate that the spectroscopic quality of MoS_2 film is very uniform. It is noted that if the original thickness of the MoO_3 layer is smaller than 2.2 nm, the MoS_2 film becomes discontinuous, where many isolated MoS_2 domains are observed (Fig. S6, ESI†).

Table 1 summarizes the thickness and morphology for the obtained MoS_2 structures upon sulfurization starting with various MoO_3 thicknesses. Also, the MoS_2 layers synthesized on sapphire are of superior quality to those obtained on SiO_2/Si substrates, and the results presented in the text were all for films synthesized on sapphire substrates. We have also performed Raman and PL characterizations for MoS_2 layers obtained from thinner MoO_3 films and the results are summarized in Fig. S7 (ESI†). In general, the Raman wavenumber value increases and the PL peak position red shifts with the initial MoO_3 thickness, consistent with the reported trend for those obtained from exfoliated MoS_2 layers.

Table 1 Effect of MoO_3 thickness on the morphology of resulting MoS_2

Thickness of MoO_3	Thickness of the obtained MoS_2	
0.8 nm	1.52 nm (2 layers)	Isolated domains
1.5–2.2 nm	1.5–2.2 nm (2–3 layers)	Isolated domains
3.6 nm	1.8–2.0 nm (3 layers)	Continuous

The as-grown wafer-scale MoS_2 film on sapphire can be transferred on to arbitrary substrates such as 300 nm SiO_2 on Si (SiO_2/Si) by the PMMA-assisted transfer method, a conventionally used method for graphene transfer.[36] Fig. 5 illustrates the procedure to transfer an as-synthesized MoS_2 layer from a sapphire to a SiO_2/Si wafer.

To evaluate the electrical performance of the MoS_2 thin layers, we fabricated bottom-gate transistors by evaporating Ti/Au electrodes directly on top of the MoS_2 layers on SiO_2/Si. Fig. 6a shows the typical output characteristics (drain current I_d *vs.* drain voltage V_d) of the MoS_2 device while Fig. 6b shows the typical transfer curves (I_d *vs.* gate voltage V_g) of the device. It is noted that the FET shows typical n-type behavior, consistent with other reports.[12,30,33] The field-effect mobility of electrons was extracted based on the slope $\Delta I_d/\Delta V_g$ fitted to the linear regime of the transfer curves using the equation $\mu = (L/WC_{ox}V_d)(\Delta I_d/\Delta V_g)$, where L and W are the channel length and width and C_{ox} is the gate capacitance.[37] It is observed that the on/off current ratio for the MoS_2 device is around 10^5 and the field-effect electron mobility of the device is about 0.8 $cm^2\ V^{-1}\ s^{-1}$.

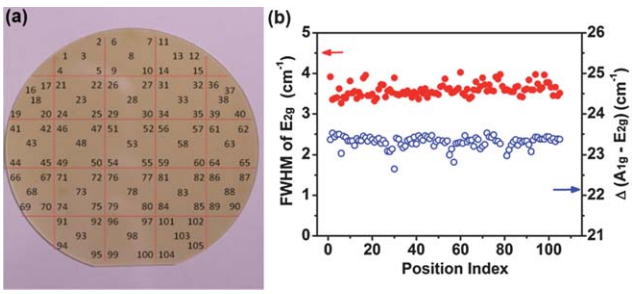

Fig. 4 (a) The numbers in the photo indicate the sites for Raman statistical measurements. (b) The statistical Δ values and the full-width at half-maximum (FWHM) of the E_{2g} peak plotted as a function of numbered site.

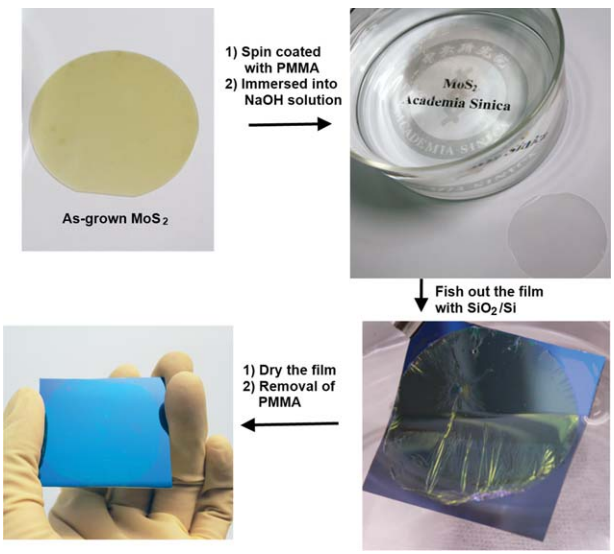

Fig. 5 Pictures showing the procedure to transfer as-synthesized MoS_2 layer from a sapphire to a SiO_2/Si wafer.

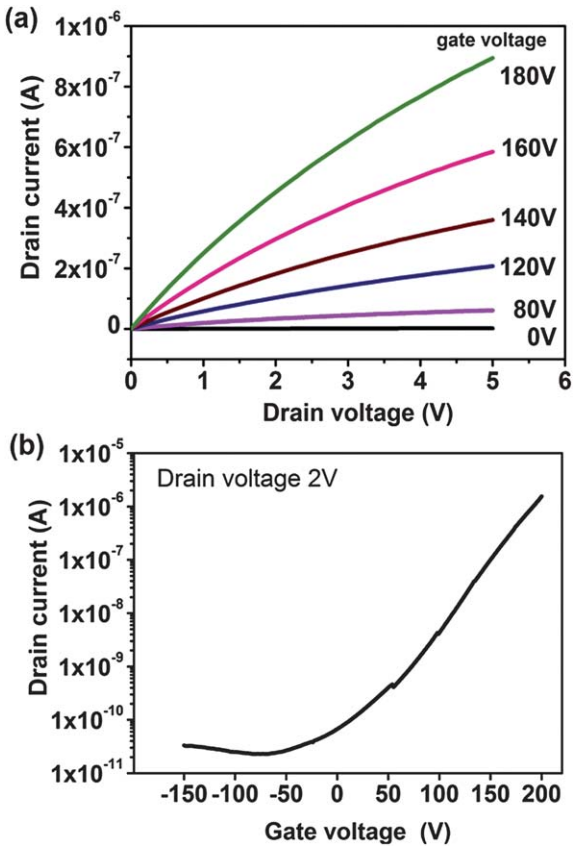

Fig. 6 (a) Output characteristics (drain current I_d *vs.* drain voltage V_d) and (b) transfer curves (I_d *vs.* gate voltage V_g) for the bottom-gate transistor based on the MoS_2 trilayer.

4. Conclusions

In conclusion, we have proposed a simple method to synthesize MoS_2 thin layers in wafer-scale by a two-step thermal process on evaporated MoO_3 layers in the presence of sulfur. Various spectroscopic and microscopy methods including Raman, PL, XPS and TEM establish the crystallinity and compositions of MoS_2 thin layers. The obtained MoS_2 thin layers are uniform in thickness and easily transferable onto arbitrary substrates. A field effect transistor fabricated with MoS_2 thin layers in a bottom gate geometry shows n-type behaviour with on/off current ratio $\sim 10^5$, and the field-effect electron mobility of the device is about 0.8 $cm^2\ V^{-1}\ s^{-1}$, comparable with the FET prepared by mechanically exfoliated MoS_2. This approach paves the large-scale route to the synthesis of MoS_2 films for future flexible electronics or optoelectronics.

Acknowledgements

This research was supported by Academia Sinica (IAMS and Nano program) and National Science Council Taiwan (NSC-99-2112-M-001-021-MY3 and 99-2738-M-001-001). L. J. Li also thanks the support from NCTU, Taiwan.

References

1 K. Novoselov, D. Jiang, F. Schedin, T. Booth, V. Khotkevich, S. Morozov and A. Geim, *Proc. Natl. Acad. Sci. U. S. A.*, 2005, **102**, 10451.
2 Y. Lin, A. Valdes-Garcia, S. Han, D. Farmer, I. Meric, Y. Sun, Y. Wu, C. Dimitrakopoulos, A. Grill, P. Avouris and K. Jenkims, *Science*, 2011, **332**, 1294–1297.
3 X. Dong, Y. Shi, W. Huang, P. Chen and L. Li, *Adv. Mater.*, 2010, **22**, 1649–1653.
4 Y. Huang, X. Dong, Y. Shi, C. Li, L. J. Li and P. Chen, *Nanoscale*, 2010, **2**, 1485–1488.
5 K. Novoselov, *Nat. Mater.*, 2007, **6**, 720.
6 N. Coleman, M. Lotya, A. O'Neill, S. Bergin, P. King, U. Khan, K. Young, A. Gaucher, S. De and R. Smith, *Science*, 2011, **331**, 568–571.
7 J. Xiao, D. Choi, L. Cosimbescu, P. Koech, J. Liu and J. P. Lemmon, *Chem. Mater.*, 2010, **22**, 4522–4524.
8 B. Radisavljevic, A. Radenovic, J. Brivio, V. Giacometti and A. Kis, *ACS Nano*, 2011, **5**, 9934–9938.
9 H. Zhong, G. Yang, H. Song, Q. Liao, H. Cui, P. Shen and C. Wang, *J. Phys. Chem. C*, 2008, **112**, 12089–12091.
10 A. Splendiani, L. Sun, Y. Zhang, T. Li, J. Kim, C. Chim, G. Galli and F. Wang, *Nano Lett.*, 2010, **10**, 1271–1275.
11 K. Mak, C. Lee, J. Hone, J. Shan and T. Heinz, *Phys. Rev. Lett.*, 2010, **105**, 136805.
12 B. Radisavljevic, A. Radenovic, J. Brivio, V. Giacometti and A. Kis, *Nat. Nanotechnol.*, 2011, **6**, 147–150.
13 J. Brivio, D. Alexander and A. Kis, *Nano Lett.*, 2011, **11**, 5148–5153.
14 H. Ramakrishna Matte, A. Gomathi, A. K. Manna, D. J. Late, R. Datta, S. K. Pati and C. N. R. Rao, *Angew. Chem., Int. Ed.*, 2010, **49**, 4059–4062.
15 C. N. R. Rao and A. Nag, *Eur. J. Inorg. Chem.*, 2010, 4244–4250.
16 K. G. Zhou, N. N. Mao, H. X. Wang, Y. Peng and H. L. Zhang, *Angew. Chem., Int. Ed.*, 2011, **50**, 10839–10840.
17 Z. Y. Zeng, Z. Y. Yin, X. Huang, H. Li, Q. Y. He, G. Lu, F. Boey and H. Zhang, *Angew. Chem., Int. Ed.*, 2011, **50**, 11093–11097.
18 P. Joensen, R. F. Frindt and R. S. Morrison, *Mater. Res. Bull.*, 1986, **21**, 457–461.
19 W. M. R. Divigalpitiya, S. R. Morrison and R. F. Frindt, *Thin Solid Films*, 1990, **186**, 177–192.
20 W. M. R. Divigalpitiya, R. F. Frindt and S. R. Morrison, *Science*, 1989, **246**, 369–371.
21 G. Eda, H. Yamaguchi, D. Voiry, T. Fujita, M. Chen and M. Chhowalla, *Nano Lett.*, 2011, **11**, 5111–5116.
22 Y. Li, H. Wang, L. Xie, Y. Liang, G. Hong and H. Dai, *J. Am. Chem. Soc.*, 2011, **133**, 7296–7299.
23 C. Altavilla, M. Sarno and P. Ciambelli, *Chem. Mater.*, 2011, **23**, 3879–3883.
24 S. Helveg, J. V. Lauritsen, E. Lægsgaard, I. Stensgaard, J. K. Nørskov, B. S. Clausen, H. Topsøe and F. Besenbacher, *Phys. Rev. Lett.*, 2000, **84**, 951–954.
25 J. V. Lauritsen, J. Kibsgaard, S. Helveg, H. Topsoe, B. S. Clausen, E. Lagsgaard and F. Besenbacher, *Nat. Nanotechnol.*, 2007, **2**, 53–58.
26 Y. Peng, Z. Meng, C. Zhong, J. Lu, W. Yu, Y. Jia and Y. Qian, *Chem. Lett.*, 2001, 772–773.
27 Q. Li, J. T. Newberg, J. C. Walter, J. C. Hemminger and R. M. Penner, *Nano Lett.*, 2004, **4**, 277–281.
28 J. Seo, Y. Jun, S. Park, H. Nah, T. Moon, B. Park, J. Kim, J. Youn and J. Cheon, *Angew. Chem., Int. Ed.*, 2007, **46**, 8828–8831.
29 S. Balendhran, J. Z. Ou, M. Bhaskaran, S. Sriram, S. Ippolito, Z. Vasic, E. Kats, S. Bhargava, S. Zhuiykov and K. Kalantar-zadeh, *Nanoscale*, 2012, **4**, 461–466.
30 Y. H. Lee, X. Q. Zhang, W. Zhang, M. T. Chang, C. T. Lin, K. D. Chang, Y. C. Yu, J. T. W. Wang, C. S. Chang, L. J. Li and T. W. Lin, *Adv. Mater.*, 2012, **24**, 2320–2325.
31 A. M. Seayad and D. M. Antonelli, *Adv. Mater.*, 2004, **16**, 765–777.
32 Y. Zhan, Z. Liu, S. Najmaei, P. M. Ajayan and L. Lou, *Small*, 2012, **8**, 966–971.
33 K. K. Liu, W. Zhang, Y. H. Lee, Y. C. Lin, M. T. Chang, C. Y. Su, C. S. Chang, H. Li, Y. Shi, H. Zhang, C. S. Lai and L. J. Li, *Nano Lett.*, 2012, **12**, 1538–1544.
34 E. Lalik, W. I. F. David, P. Barnes and J. F. C. Turner, *J. Phys. Chem. B*, 2001, **105**, 9153–9156.
35 C. Lee, H. Yan, L. E. Brus, T. F. Heinz, J. Hone and S. Ryu, *ACS Nano*, 2010, **4**, 2695–2700.
36 C. S. Chen, C. T. Lin, Y. H. Lee, K. K. Liu, C. Y. Su, W. Zhang and L. J. Li, *Small*, 2012, **8**, 43–46.
37 C. W. Lee, C. H. Weng, L. Wei, Y. Chen, M. B. Chan-Park, C. H. Tsai, K. C. Leou, C. H. P. Poa, J. Wang and L. J. Li, *J. Phys. Chem. C*, 2008, **112**, 12089–12091.